

**Structure-based theoretical characterisation
of the redox-dependent titration behaviour
of cytochrome bc_1**

Dissertation zur Erlangung der Doktorwürde
der Fakultät für Biologie, Chemie und Geowissenschaften
der Universität Bayreuth

vorgelegt von
Astrid Klingen

November 2006

Ich erkläre hiermit, dass ich die vorliegende Arbeit selbstständig verfasst und keine anderen als die angegebenen Quellen und Hilfsmittel verwendet habe. Ich erkläre des Weiteren, dass ich weder diese noch eine gleichartige Doktorprüfung an einer anderen Hochschule endgültig nicht bestanden habe.

Bayreuth, 15. Februar 2007

Die vorliegende Arbeit wurde in der Zeit vom Januar 2004 bis November 2006 an der Universität Bayreuth unter der Leitung von Prof. Dr. Matthias Ullmann angefertigt.

Vollständiger Abdruck der von der Fakultät für Biologie, Chemie und Geowissenschaften der Universität Bayreuth genehmigten Dissertation zur Erlangung des akademischen Grades Doktor der Naturwissenschaften (Dr. rer. nat.)

Datum der Einreichung der Arbeit: 2. 11. 2006

Datum des wissenschaftlichen Kolloquiums: 23. 1. 2007

Prüfungsausschuss: Prof. Dr. Matthias Ullmann (Erstgutachter)
Prof. Dr. Holger Dobbek (Zweitgutachter)
Prof. Dr. Benedikt Westermann (Vorsitzender)
Prof. Dr. Matthias Ballauff

Mein herzlicher Dank geht an

Prof. Dr. Matthias Ullmann für die ausgezeichnete und intensive wissenschaftliche Betreuung meiner Arbeit sowie für die hervorragenden Arbeitsbedingungen in seiner Gruppe.

Timm Essigke für die äußerst kompetente und hilfreiche Unterstützung in allen Rechnerangelegenheiten.

meinen Kollaborationspartnern, insbesondere Lars Schäfer und Dr. Carola Hunte, für die erfolgreiche und teilweise anregende Zusammenarbeit.

Dr. Torsten Becker, meinen Eltern und Eva Krammer für inhaltliches und formales Korrekturlesen.

dem Boehringer Ingelheim Fonds mit Frau Dr. Claudia Walther und Frau Monika Beutelspacher für die finanzielle und ideelle Unterstützung meiner Arbeit.

meinen Kollegen, insbesondere Torsten, Eva und Edda, für ihre Hilfe bei der täglichen Arbeit und viel gute Gesellschaft in und außerhalb der B14.

meiner Familie und meinen Freunden für ihre kleinen und großen Beiträge zum Gelingen dieser Arbeit.

Inhaltsverzeichnis

Zusammenfassung	4
Abstract	5
List of Abbreviations	6
Function, structure and mechanism of cytochrome bc_1	7
Cytochrome bc_1 in mitochondrial respiration	7
Subunit composition and mechanism of cytochrome bc_1	8
Structure of cytochrome bc_1 from <i>Saccharomyces cerevisiae</i>	10
The Q_i -site	11
The Q_o -site	12
Theoretical investigation of the titration behaviour of proteins	15
Poisson-Boltzmann electrostatics	15
Calculation of protonation state energies	16
Metropolis Monte Carlo sampling of protonation state energies	18
Monte Carlo titration calculations with conformational variability	19
Quantum chemical characterisation of protonation equilibria in vacuum	21
Synopsis of published and submitted manuscripts	23
Irregular titration behaviour of individual sites in proteins	23
Coupling between conformational and protonation state changes in asFP	24
pH-dependence of the position of CoQ_B in the photosynthetic reaction centre	24
Coupling between redox and protonation reactions of the Rieske cluster	25
Redox-linked protonation state changes in cytochrome bc_1	26
Bibliography	28
List of published and submitted manuscripts	35
Manuscript A	37
Manuscript B	38
Manuscript C	39
Manuscript D	40
Manuscript E	41
Manuscript F	42

Zusammenfassung

Cytochrom bc_1 ist eine Coenzym Q-Cytochrom c -Oxidoreduktase. Es fungiert als Komplex III der mitochondrialen Atmungskette, deren Komponenten in die innere Mitochondrienmembran eingebettet sind. Cytochrom bc_1 koppelt die Elektronentransferreaktion zwischen Coenzym Q (CoQ) und Cytochrom c an die gerichtete Bewegung von Protonen über die Membran, und wandelt so die chemische Energie des reduzierten CoQ in eine protonenmotorische Kraft um. Die Kopplung der beiden Prozesse in Cytochrom bc_1 beruht auf dem sogenannten Q-Zyklus. Grundlage dieses Mechanismus sind zwei aktive Zentren, die auf entgegengesetzten Seiten der Membran die Oxidation/Deprotonierung beziehungsweise die Reduktion/Protonierung von CoQ katalysieren. Die genaue Mechanismus dieser katalytischen Reaktionen ist nicht verstanden. Die vorliegende Arbeit stellt daher einen strukturbasierten theoretischen Ansatz vor, mit dem redoxabhängige Protonierungszustandsänderungen in Cytochrom bc_1 identifiziert werden können. Cytochrom bc_1 stellt wegen seiner Membranumgebung, seiner zahlreichen titrierbaren Gruppen, ihrer Wechselwirkungen untereinander und mit redoxaktiven Kofaktoren, sowie wegen seiner konformationellen Variabilität ein kompliziertes System dar. In einer Reihe von vier Arbeiten an einfacheren Systemen wurden zunächst Lösungen für diese Probleme entwickelt. Die erste Arbeit charakterisiert den Einfluss von elektrostatischer Wechselwirkung und konformationeller Variabilität auf das Protonierungsverhalten von fiktiven Modellsystemen (Manuskript A). Die Kopplung von Konformations- und Protonierungszustandsänderungen wurde dann in einem relativ einfachen Protein untersucht (Manuskript B). Die pH-Abhängigkeit der Bindungsstelle von CoQ im aktiven Zentrum eines CoQ-reduzierenden Transmembranproteins wird in Manuskript C beschrieben. Manuskript D charakterisiert die Redox- und Protonierungsreaktionen des Rieske Eisen-Schwefel-Zentrums, das eine der prosthetischen Gruppen von Cytochrom bc_1 darstellt. Auf der Grundlage von Kristallstrukturen von Cytochrom bc_1 aus *Saccharomyces cerevisiae* wurden schließlich die Protonierungswahrscheinlichkeiten aller titrierbaren Gruppen im vollständig oxidierten und vollständig reduzierten Protein berechnet. Dadurch lassen sich einzelne Gruppen identifizieren, deren Protonierungszustand sich in Abhängigkeit vom Redoxzustand des Systems verändert. Die Ergebnisse zeigen Übereinstimmung mit experimentellen Daten und helfen bei der Interpretation redoxinduzierter Veränderungen in komplizierten Infrarot-Spektren. In Manuskript E wird ein neuer Weg der Protonenaufnahme während der CoQ-Reduktion vorgeschlagen. Die Ergebnisse für das CoQ-oxidierende Zentrum (Manuskript F) sind vereinbar mit einem viel diskutierten Mechanismus, der die Reaktion nur dann zulässt, wenn schädliche Nebenreaktionen nicht stattfinden können. Eine Kopplung von Reduktion und Protonierung des Rieske-Zentrums sowie des Häm b_L unterstreicht die Bedeutung dieser Gruppen in der konzertierten Oxidation/Deprotonierung von CoQ.

Abstract

Cytochrome bc_1 is a coenzyme Q-cytochrome c -oxidoreductase that represents complex III of the mitochondrial respiratory chain. It spans the inner mitochondrial membrane and uses the free energy of electron transfer from coenzyme Q (CoQ) to cytochrome c to shift protons across the membrane. The chemical energy of reduced CoQ is thus converted into the energy of a proton motive force. The coupling between electron transfer and proton translocation is based on the Q-cycle mechanism. This mechanism comprises two CoQ-binding active sites, that catalyse the oxidation/deprotonation and reduction/protonation of CoQ, respectively. The two sites are located at opposite sides of the membrane. Their intricate chemistry is a matter of ongoing debate. This thesis describes a structure-based theoretical approach to characterise redox-linked protonation state changes in cytochrome bc_1 , that are at the heart of its catalytic mechanism. The analysis of the titration behaviour of cytochrome bc_1 is however complicated by its membrane environment, its high number of titratable sites, their interaction with each other and with redox-active groups, and the conformational variability of the CoQ oxidation site. A series of four studies has prepared the grounds to approach this challenging system. The first article analyses the effect of conformational variability and electrostatic interaction on the titration behaviour of simple model systems (Manuscript A). Based on this study, the coupling between conformational and protonation state changes has been analysed in a relatively simple soluble protein (Manuscript B). The effect of pH on the position of CoQ in a CoQ-reducing transmembrane protein has been quantified as described in Manuscript C. Manuscript D presents a study of the coupling between redox and protonation reactions of the Rieske iron-sulphur cluster, that is one of the prosthetic groups of cytochrome bc_1 . Based on crystal structures of cytochrome bc_1 from *Saccharomyces cerevisiae*, the protonation probabilities of all titratable groups in the protein have then been calculated, once for its completely oxidised state and once for its completely reduced state. The results allow to identify individual residues that undergo redox-linked protonation state changes. They are consistent with the results of Fourier transform infra-red spectroscopy, and aid in the often complicated interpretation of these experimental data. The calculation results reveal a modified path for proton uptake to the CoQ reduction site (Manuscript E). In the CoQ oxidation site (Manuscript F), the population of protonation and conformational states is consistent with a previously proposed gating mechanism of the catalytic reaction, that may help to prevent harmful bypass reactions. Coupling between the reduction and protonation of both the Rieske cluster and haem b_L highlight the importance of these cofactors in the combined oxidation and deprotonation of CoQ.

List of Abbreviations

ADP	adenosine diphosphate
ATP	adenosine triphosphate
CDL	cardiolipin
CoQ	coenzyme Q
CoQ _B	coenzyme Q bound in the Q _B -site of the photosynthetic reaction centre
CYB	cytochrome <i>b</i>
CYC1	cytochrome <i>c</i> ₁
DFT	density functional theory
HDBT	hydroxydioxobenzothiazole
ISP	Rieske iron-sulphur protein
FTIR	Fourier transform infra-red spectroscopy
MC	Monte Carlo
NADH	reduced nicotine-adenine dinucleotide
NMR	nuclear magnetic resonance spectroscopy
PBE	Poisson-Boltzmann electrostatics
PDB	Brookhaven Protein Data Bank (www.rcsb.org/pdb)
Q	oxidised and deprotonated CoQ
QH ₂	reduced and protonated CoQ
QH·	singly protonated semiquinone form of CoQ
Q _B -site	coenzyme Q reduction site of the photosynthetic reaction centre
Q _i -site	coenzyme Q reduction site of cytochrome <i>bc</i> ₁
Q _o -site	coenzyme Q oxidation site of cytochrome <i>bc</i> ₁
STED	stimulated emission depletion
SU	subunit

1 Function, structure and mechanism of cytochrome bc_1

Cytochrome bc_1 in mitochondrial respiration. Cytochrome bc_1 is a multi-subunit transmembrane protein complex, that transfers electrons from a lipophilic quinol compound to a small haem protein, and simultaneously translocates protons across the membrane [1]. This process is central to the electron transfer chains of mitochondrial and prokaryotic respiration, as well as of bacterial photosynthesis.

Mitochondrial cytochrome bc_1 represents complex III of the respiratory chain. In eukaryotic cells it is located in the inner mitochondrial membrane and transfers electrons from reduced coenzyme Q (CoQ) to cytochrome c (Fig. 1). CoQ is a lipophilic compound that moves within the membrane, it delivers electrons from complexes I and II to cytochrome bc_1 . Cytochrome c is a hydrophilic protein located in the intermembrane space. It carries electrons from cytochrome bc_1 to complex IV, where electrons are transferred to the final electron acceptor oxygen.

The overall electron transfer from NADH and succinate to molecular oxygen through CoQ, cytochrome c and the complexes of the respiratory chain is an energetically favourable process. Complex I, III and IV couple electron transfer to the translocation of protons from the mitochondrial matrix into the intermembrane space. The energy of electron transfer is thus converted into the energy of a proton motive force. ATP-synthase exploits this proton motive force: protons move back into the the mitochondrial matrix along their concentration gradient and thereby drive ATP-synthesis. The overall process of electron transfer and ATP-synthesis, coupled via generation and utilisation of a proton motive force, is known as oxidative phosphorylation [2, 3]. Ref. 4 provides a historical outline of the discovery of the mitochondrial cytochromes by Keilin, their identification

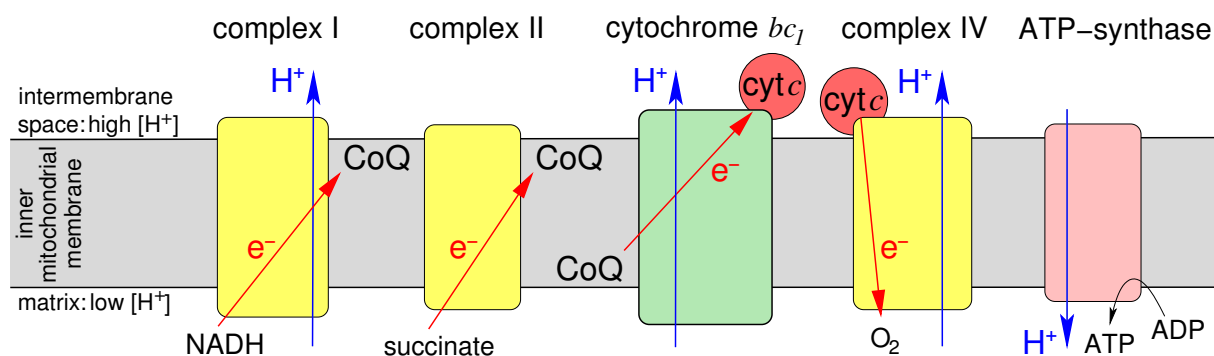


Figure 1. Cytochrome bc_1 is complex III of the mitochondrial respiratory chain. Electrons enter the chain via oxidation of NADH and succinate by complex I and II, respectively. CoQ and cytochrome c are the mobile components that transfer electrons between the large transmembrane complexes. Oxygen is the final electron acceptor. Complex I, III and IV use the energy of electron transfer to translocate protons across the membrane. ATP-synthase exploits the resulting proton motive force to produce ATP from ADP and inorganic phosphate.

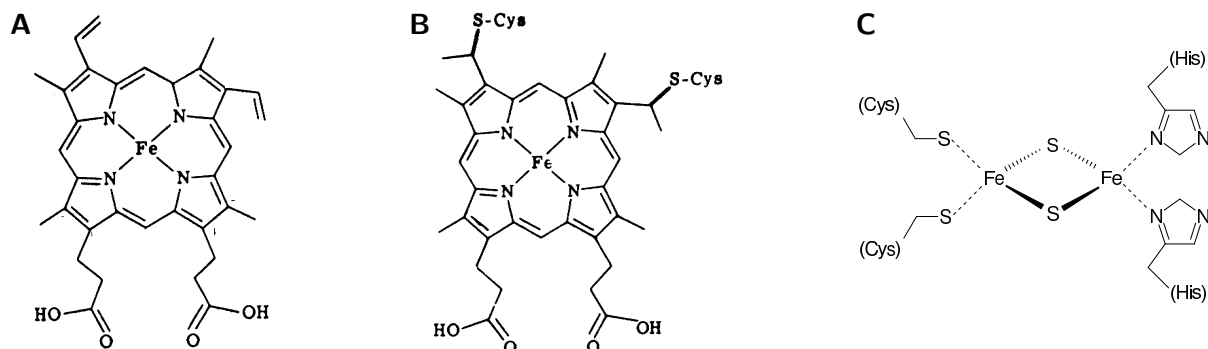


Figure 2. Chemical structure of the redox-active cofactors of cytochrome bc_1 . **A)** b -type haem where axial iron ligands would be two histidines [1]. **B)** c -type haem where axial iron ligands would be one histidine and one methionine [1]. **C)** The Rieske iron-sulphur cluster.

with Warburg's "Atmungsferment" and their separation into the components of complex III and IV of the respiratory chain.

Subunit composition and mechanism of cytochrome bc_1 . Cytochrome bc_1 consists of three essential catalytic subunits. Cytochrome b is the largest of the three, it consists of eight transmembrane helices and binds two b -type haem groups (Fig. 2A), named haem b_L and b_H . Cytochrome c_1 is anchored to the membrane by a single transmembrane helix. Its hydrophilic head domain, located in the intermembrane space, contains a c -type haem group (Fig. 2B) called haem c_1 . The Rieske iron-sulphur protein (ISP) also consists of a single transmembrane helix and a hydrophilic head domain in the intermembrane space. The ISP head domain binds a Rieske Fe_2S_2 iron-sulphur cluster (Fig. 2C). In addition to the catalytic core of cytochrome b , cytochrome c_1 and the Rieske ISP, cytochrome bc_1 complexes from different organisms contain up to eight additional subunits.

The three essential subunits of cytochrome bc_1 catalyse electron transfer from reduced CoQ to cytochrome c . While cytochrome c is a haem protein and undergoes relatively simple one-electron redox transitions, CoQ exists in many different redox and protonation

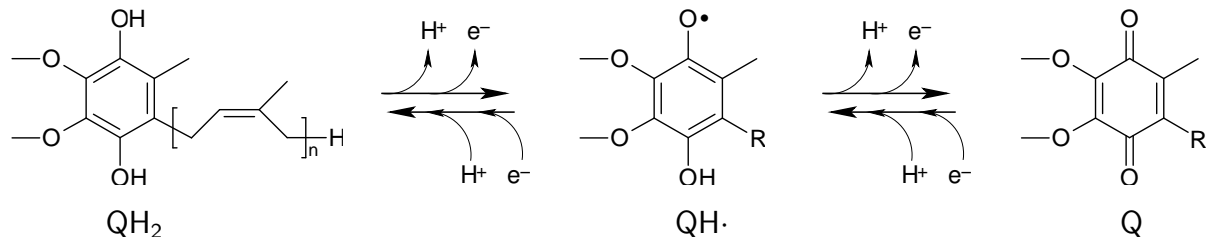


Figure 3. Interconversion between the quinol (QH_2) and quinone (Q) forms of mitochondrial CoQ. The singly protonated semiquinone radical ($QH\cdot$) is one of the possible intermediates. CoQ can in principle exist in nine different combinations of redox and protonation forms. The hydrophobic tail contains a varying number of isoprenoid units.

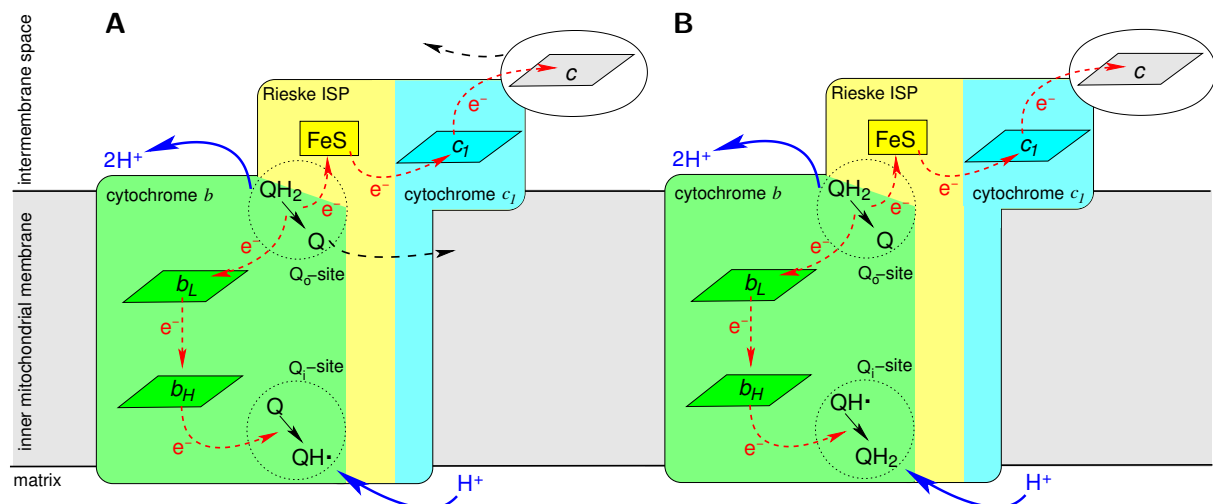


Figure 4. The Q-cycle mechanism of cytochrome bc_1 . **A)** During the first half of the cycle, an electron from the oxidation of quinol (QH_2) in the Q_o -site is transferred via haem b_L and b_H to the the Q_i -site, where quinone (Q) is reduced to form a stable semiquinone intermediate ($QH\cdot$). **B)** In the second half of the cycle, the semiquinone in the Q_i -site gets reduced to quinol. In both halves of the cycles, one electron from the oxidation of CoQ is transferred to cytochrome c via the Rieske iron-sulphur cluster (FeS) and haem c_1 . Release of the products of the first half of the cycle (oxidised CoQ and reduced cytochrome c) is indicated by black dashed arrows.

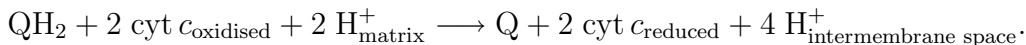
states. Upon complete oxidation of CoQ, two electrons and two protons are set free (Fig. 3). The singly protonated semiquinone radical is one of the possible intermediates of this reaction.

The coupling between electron transfer and proton translocation in cytochrome bc_1 is described by the so-called modified Q-cycle mechanism (Fig. 4). Cytochrome bc_1 has two CoQ binding sites: the Q_o -site catalyses CoQ oxidation, the Q_i -site catalyses CoQ reduction. When reduced CoQ gets oxidised in the the Q_o -site, two electrons are set free that are transferred to two different electron acceptors: one electron is transferred to the Rieske cluster, the other one to haem b_L . This unusual process is referred to as bifurcation of electron transfer pathways in the Q_o -site. From the Rieske cluster, the electron is transferred via haem c_1 to the substrate and final electron acceptor cytochrome c . In order to transfer the electron from CoQ to haem c_1 , the ISP subunit undergoes a conformational change with its head domain moving from the Q_o -site interface with cytochrome b to an interface with cytochrome c_1 .

From haem b_L , electrons are transferred via haem b_H towards the Q_i -site. In the Q_i -site, CoQ is reduced by two electrons arriving sequentially from the Q_o -site. The semiquinone radical is a stable intermediate in this two electron reduction reaction in the Q_i -site [5, 6].

Since the Q_o -site has to turn over twice in order to fully reduce CoQ in the Q_i -site,

the overall reaction catalysed by cytochrome bc_1 is



The strict coupling between the reduction/protonation and oxidation/deprotonation of CoQ, together with the location of the sites of CoQ oxidation and reduction at different sides of the membrane, leads to the coupling between electron transfer and proton translocation in cytochrome bc_1 . In total, half of the electrons from CoQ oxidation in the Q_o -site are transferred back into the pool of reduced CoQ via transfer to the Q_i -site. Unlike cytochrome c oxidase, cytochrome bc_1 is not a true proton pump, it rather functions by a mechanism similar to the vectorial redox-loop mechanism proposed by Mitchell [7]: electron transfer from the Q_o -site to the Q_i -site is the main electrogenic process while reduced CoQ serves as hydrogen carrier between the two active sites. Ref. 8 gives an account of the historical development of the Q-cycle concept. Ref. 9 reviews the Q-cycle basics as they are generally accepted today.

The structure of cytochrome bc_1 from *Saccharomyces cerevisiae*. The structure of cytochrome bc_1 from the yeast *Saccharomyces cerevisiae* has been solved by X-ray crystallography (Fig. 5A). The complex was crystallised with the Q_o -site inhibitor stigmatellin (2.3 Å resolution, PDB-code 1KB9) [10, 11] and with the Q_o -site inhibitor hydroxydioxobenzothiazole (HDBT, 2.5 Å resolution, PDB-code 1P84) [12, 13]. In both structures, the Q_i -site contains the substrate CoQ and the Rieske head domain is located at its Q_o -site interface with cytochrome b . Crystallisation of the complex was brought about by binding of an antibody fragment to the Rieske head domain [14]. The complex has a molecular weight of about 470 kDa.

Cytochrome bc_1 is a dimer, meaning that it contains two copies of each of the different subunits. The subunits of each half of the complex are arranged in two bundles of transmembrane helices. The functionality of the dimeric state of the complex is most obvious from the positioning of the Rieske subunit: the head domain forms the Q_o -site at an interface with cytochrome b from one monomer, but its transmembrane anchor is part of the helix bundle of the other monomer. In addition, the dimeric structure may allow for mechanistically relevant inter-monomer electron transfer or a half-of-the-sites regulation of activity [15–19].

Besides the three catalytic subunits, cytochrome bc_1 from *S. cerevisiae* contains seven additional subunits. These non-catalytic subunits are not involved in electron transfer but they contribute to the stability of the complex. The two so-called core subunits [20] make up for the large part of the complex located in the mitochondrial matrix (Fig. 5A). They bear homology to soluble heterodimeric zinc-dependent metalloproteases [21]. The small and loosely bound subunit 10 is missing in the structures of cytochrome bc_1 from

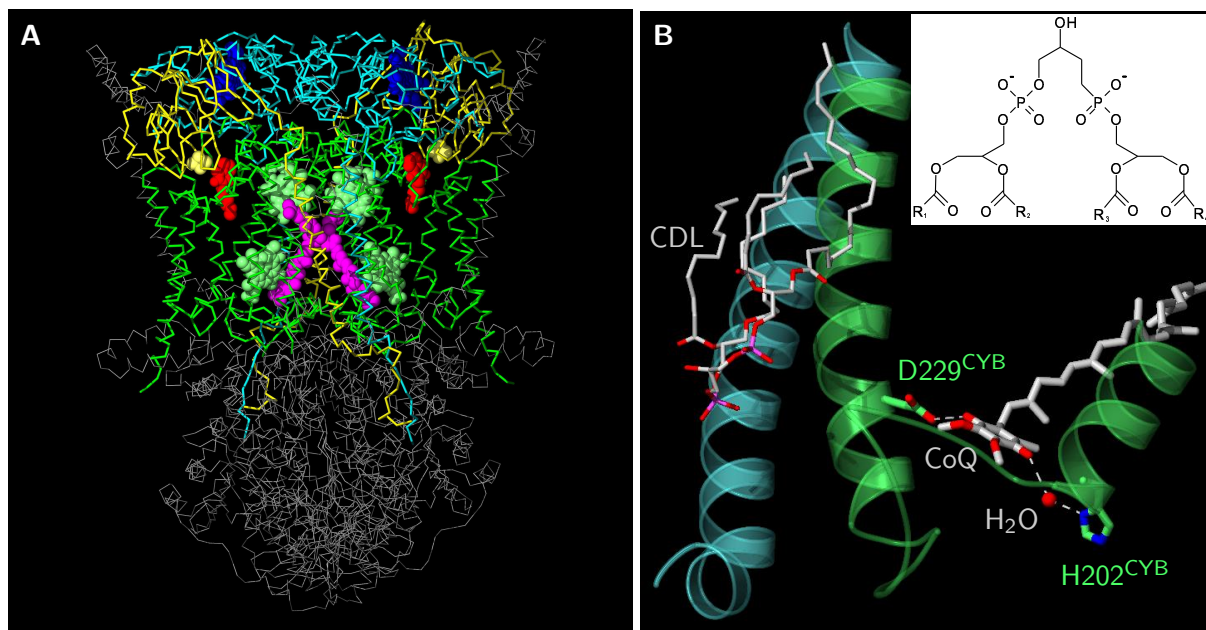


Figure 5. **A)** The structure of cytochrome bc_1 from *S. cerevisiae* as solved by X-ray crystallography [12]. Cytochrome b (green) makes up for most of the transmembrane part of the complex. The hydrophilic head domains of cytochrome c_1 (turquoise) and the ISP (yellow) are located in the intermembrane space. The redox cofactors are depicted in green (haem b_L and b_H), blue (haem c_1) and yellow spheres (iron-sulphur cluster). The substrate CoQ in the Q_i -site is coloured in magenta, the inhibitor HDBT in the Q_o -site is coloured in red. The non-catalytic subunits are shown in grey. **B)** The Q_i -site. Sidechains and a water molecule that coordinate CoQ are highlighted. Hydrogen bond interactions are shown as dashed lines. Non-carbon atoms are shown in standard colours. A cardiolipin molecule (CDL) is bound close to the Q_i -site. Its chemical structure is shown as inset.

S. cerevisiae, since it is lost during the purification procedure. In the following, specific residues in cytochrome bc_1 from *S. cerevisiae* are denoted by their single letter amino acid code, their residue number, and a subunit identifier (CYB – cytochrome b ; CYC1 – cytochrome c_1 ; ISP – Rieske iron-sulphur subunit; SU1, SU2, SU6, SU7, SU8, SU9 – non-catalytic subunits 1, 2 and 6 to 9).

The Q_i -site. The Q_i -site catalyses the reduction of CoQ (Fig. 3, right to left). This two-electron reaction proceeds in two steps because the electrons arrive sequentially from two separate CoQ oxidation reactions in the Q_o -site (Fig. 4). The semiquinone form of CoQ is a stable intermediate of the Q_i -site reaction [5, 6].

The crystal structures of cytochrome bc_1 from *S. cerevisiae* contain CoQ in the Q_i -site and reveal its binding mode in the active site (Fig. 5B). D229^{CYB} is a direct ligand of CoQ and has been proposed to be a primary proton donor group during the CoQ reduction reaction [10, 14, 22]. The interaction between H202^{CYB} and CoQ is mediated by a water molecule. Different patterns of water molecules interacting with CoQ have been observed

in the Q_i -sites of yeast, bovine and chicken cytochrome bc_1 [10,22–24]. It is a matter of ongoing debate, whether the presence and absence of water between H202^{CYB}, D229^{CYB} and CoQ represent different mechanistically relevant states of the Q_i -site [10,14,22,25,26].

The preparations of cytochrome bc_1 from different organisms all contain tightly bound lipids [11,13]. Cardiolipin (CDL) in particular has been shown to be essential for the function of cytochrome bc_1 [27]. CDL is a dianionic lipid (Fig. 5B, inlay) that is exclusively found in the inner mitochondrial membrane and in evolutionary related bacterial plasma membranes [28]. In the structures of cytochrome bc_1 from *S. cerevisiae*, two CDL molecules have been cocrystallised, one of them is located close to the Q_i -site (Fig. 5B). It has been proposed that CDL may play a role in proton uptake to the Q_i -site [10,11,29].

The Q_o -site. The Q_o -site is the primary site of energy conversion of cytochrome bc_1 . The rather complicated chemistry of CoQ oxidation in this site is poorly understood and has been a matter of debate for decades [30–32]. Ongoing discussion deals with the position of CoQ in the active site, the nature of proton acceptor groups, the timing of the individual electron and proton transfer steps, and the conformational change of the Rieske subunit.

In all known structures of cytochrome bc_1 , the Q_o -site is either empty or occupied by different inhibitors [10,12,22–24,33–37]. The inhibitors can be classified as “distal” or “proximal” depending on their binding position relative to haem b_L . Both stigmatellin and HDBT, the inhibitors cocrystallised with cytochrome bc_1 from *S. cerevisiae*, bind distally to haem b_L and interact directly with the Rieske cluster (Fig. 6). Stigmatellin and HDBT apparently represent analogues of the neutral and negatively charged semiquinone form of CoQ, respectively. The substrate CoQ most likely binds in the same position as stigmatellin and HDBT at least until transfer of the first electron towards the Rieske cluster is accomplished [38]. Based on the observation of a different binding position for the proximal inhibitors, it has been proposed that CoQ may move from a distal towards a proximal position during the catalytic reaction in the Q_o -site [39,40]. Alternatively, the two binding positions may be occupied simultaneously by two different molecules of CoQ [41–44]. Evidence for the functional significance of both the moving semiquinone and the double occupancy model have however remained sparse.

The tight interaction of the Rieske cluster with the Q_o -site inhibitors apparently seals the site from the aqueous phase of the intermembrane space. The protons dissociating from CoQ upon its oxidation therefore have to be transferred to proton acceptor groups in the site and can only later be set free to the intermembrane space, most likely after the conformational change of the ISP. The hydrogen bond between the inhibitors and H181^{ISP} observed in the crystal structures (Fig. 6) supports the previously proposed idea, that CoQ may transfer a proton to this ligand histidine upon electron transfer to the

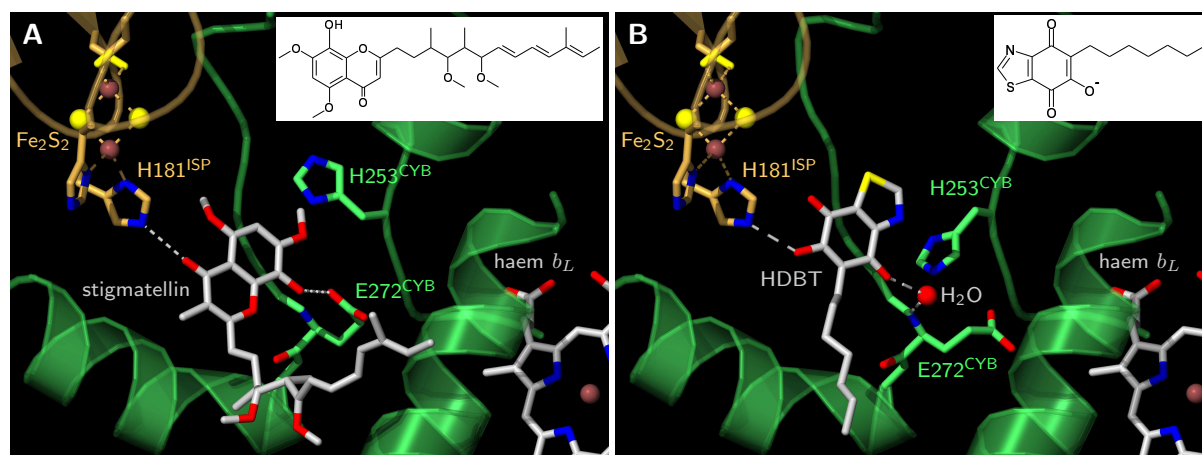


Figure 6. The Q_o -site of cytochrome bc_1 from *S. cerevisiae* with **A)** stigmatellin [11] and **B)** HDBT [12]. The ISP subunit is shown in ochre, the iron-sulphur cluster with its ligand cysteine and histidine residues is highlighted. In the cytochrome b subunit (green), sidechains that adopt different conformations in presence of the different inhibitors are highlighted. The interaction between the backbone of E272^{CYB} and HDBT is mediated by a water molecule. Hydrogen bond interactions are shown as dashed lines. Non-carbon atoms are shown in their standard colour code. The chemical structures of the inhibitors are shown as inlays.

iron-sulphur cluster [45–48]. E272^{CYB}, which forms a hydrogen bond towards stigmatellin (Fig. 6A), has been discussed as possible second proton acceptor group [29, 32, 49, 50].

Although stigmatellin and HDBT bind in very similar positions in cytochrome bc_1 from *S. cerevisiae*, they introduce different conformations of a limited number of Q_o -site residues. Stigmatellin interacts closely with the sidechain of E272^{CYB}, whereas this sidechain is rotated out of the binding pocket in cytochrome bc_1 crystallised with HDBT (Fig. 6). This conformational variability of E272^{CYB} has been proposed to have functional relevance and has been included into different detailed mechanistic schemes of Q_o -site catalysis [29, 32, 49, 50]. However, recent mutational studies have questioned the role of this residue in redox-linked proton transfer in the Q_o -site [51, 52]. Instead, E272^{CYB} may be involved in gating of the CoQ oxidation reaction, that has been postulated to prevent harmful bypass reactions [52–54]. Such bypass reactions must be efficiently controlled, because they can lead to the production of oxygen radicals that can seriously damage vital cellular structures [55–60]. While research on cytochrome bc_1 has for long been directed towards elucidating the timing of electron and proton transfer events in the Q_o -site the focus has during the last two years slightly shifted towards identifying a mechanism that accounts for the reversibility of the Q_o -site reactions while simultaneously explaining the control of bypass reactions. The precise design of the postulated gating of CoQ oxidation in cytochrome bc_1 is a matter of ongoing debate [50, 52–54, 61].

A key factor in all prevailing formulations of the Q_o -site mechanism is the conformational change of the ISP. In the crystal structures of cytochrome bc_1 from chicken, the

Rieske head domain was found to populate two different positions: a *b*-position forming the Q_o-site together with cytochrome *b*, and a *c*₁-position with the Rieske cluster close to haem *c*₁ [23]. During turnover of cytochrome *bc*₁, the Rieske head domain moves between its *b* and *c*₁ position to accomplish electron transfer from the Q_o-site to haem *c*₁ [62,63]. The domain movement can be described as a 56° rotation of the relatively inflexible head domain relative to the transmembrane helix of the ISP subunit [64]. The same region of the Rieske head domain surrounding the exposed iron-sulphur cluster interacts with both cytochrome *b* and cytochrome *c*₁. In mutational studies, the flexibility of a linker region between transmembrane helix and head domain has been shown to be essential for the conformational change [65–68]. The redox state of the iron-sulphur cluster [69–72], binding of inhibitors [36,73] and shape complementarity of cytochrome *b* and the ISP [74] have been shown to control the position of the ISP head domain.

2 Theoretical investigation of the titration behaviour of proteins

Proteins contain many titratable sites that can bind or release protons in dependence of the proton concentration in the surrounding medium. Such titratable sites are for instance the sidechains of amino acids such as – amongst others – glutamate, histidine and lysine, but also the carboxy- and amino-termini of the polypeptide chains, and protonatable groups of certain cofactors. Changes in the protonation state of proteins affect their charge distribution: for example, protonation of a titratable site can introduce a positive charge, or it can neutralise an existing negative charge. Since electrostatics are an important physical basis of enzymatic catalysis [75], it is essential to understand the protonation behaviour of proteins in order to infer how enzymes work. The importance of electrostatics is particularly evident for enzymes that catalyse the charge transfer reactions involved in cellular energy conversion.

Protonation state changes of complex systems such as proteins are difficult to quantify experimentally. Calorimetric experiments assess only the macroscopic protonation state of a protein: they detect the release or uptake of a proton at a certain pH but can not identify the individual titratable sites that are responsible for the change in protonation. Nuclear magnetic resonance (NMR) experiments can detect changes in the protonation form of individual residues but are applicable only to systems that are much smaller than the charge-transferring transmembrane complexes of cellular energy conversion. Fourier transform infra-red (FTIR) spectroscopy can detect changes in the protonation form of a certain type of titratable sites as for instance carboxylic sidechains, but the assignment to an individual residue is often difficult. In the following, a theoretical framework will be described that allows to precisely quantify the protonation behaviour of proteins and their individual sites, and can thus provide an important complement to experimental assays.

Poisson-Boltzmann electrostatics. In the framework of Poisson-Boltzmann electrostatics (PBE), a semi-macroscopic picture is used to describe the system of interest. Atomic partial charges located at the position of each individual atom are used to describe the charge distribution $\rho_{\text{protein}}(\vec{r})$. \vec{r} describes a point in space. The effect of mobile charges around the protein is accounted for by assuming a Boltzmann distribution of these ions in the potential of the protein. Polarisation effects are accounted for by the assignment of different dielectric constants ϵ . The dielectric constant of a medium quantifies the electrostatic screening of a charge in this medium. Typically, a dielectric constant of 80 is used for aqueous media, while a value of 4 is used for proteins [76], reflecting the lower degree of polarisability for the protein compared to water. The spatial distribution of dielectric media $\epsilon(\vec{r})$ is commonly determined from the coordinates and radii of the

protein atoms: the volume that is occupied by the protein is assigned $\epsilon_{\text{protein}}$, while everything else is assigned ϵ_{water} . A method to treat a membrane environment within this framework is described in Ref. 77.

For a system characterised by a distribution of different dielectric media $\epsilon(\vec{r})$ and charges $\rho_{\text{protein}}(\vec{r})$, the electrostatic potential $\phi(\vec{r})$ can be obtained from the solution of the linearised Poisson-Boltzmann equation

$$\vec{\nabla}[\epsilon(\vec{r})\vec{\nabla}\phi(\vec{r})] = \frac{1}{\epsilon_0} \left(\rho_{\text{protein}}(\vec{r}) + \sum_i^I \left(\frac{c_i z_i^2 e^2}{RT} \phi(\vec{r}) \right) \right), \quad (1)$$

where c_i is the concentration of ions of type i , z_i is their unitless formal charge and $e = 1.602 \cdot 10^{-19}$ As is the elementary charge. The summation runs over I different types of ions. R is the universal gas constant and T the temperature. The formulation of Eq. 1 is valid if the sum of the charges of all ions is zero and if the energy of the ions in the protein's electrostatic potential is small compared to RT .

Calculation of protonation state energies. Proteins commonly contain many titratable sites that can be either protonated or deprotonated. Such a system with N titratable sites can adopt a total of 2^N different microscopic protonation states n . These protonation states are characterised by a protonation state vector $\vec{x}^{(n)}$ where the components x_i are 1 or 0, depending on whether site $i = 1, \dots, N$ is protonated or deprotonated, respectively. At a given $\text{pH} = -\lg[\text{H}^+]$, each of the protonation states has a different protonation state energy $G^{(n)}$:

$$G^{(n)}(\text{pH}) = \sum_i^N (x_i^{(n)} - x_i^{(0)}) (\text{pH} - \text{p}K_i^{\text{intr}}) + \frac{1}{2} \sum_i^N \sum_j^N (x_i^{(n)} - x_i^{(0)}) (x_j^{(n)} - x_j^{(0)}) W_{i,j}. \quad (2)$$

Here, $G^{(n)}$ is the energy of protonation state $n = 0, \dots, 2^N - 1$ relative to the energy of a reference protonation state $G^{(0)}$. $x_i^{(0)}$ stands for the protonation form of site i in the reference protonation state. $\text{p}K_i^{\text{intr}}$ is the intrinsic $\text{p}K$ of site i , that is the $\text{p}K$ that site i would have if all other sites were in their reference protonation form. $W_{i,j}$ is the interaction energy between two sites i and j . In the formulation of all equations in this section it is assumed that all energies are in $\text{p}K$ -units, which convert to kcal/mol by multiplication with $1/RT \ln 10$.

The intrinsic $\text{p}K$ is calculated as shift relative to a model compound $\text{p}K$ value upon transfer of an appropriate model compound from aqueous solution to the protein environment (Fig. 7A):

$$\text{p}K^{\text{intr}} = \text{p}K^{\text{model}} + \Delta G_{\text{trans}}(\text{A}^-) - \Delta G_{\text{trans}}(\text{AH}). \quad (3)$$

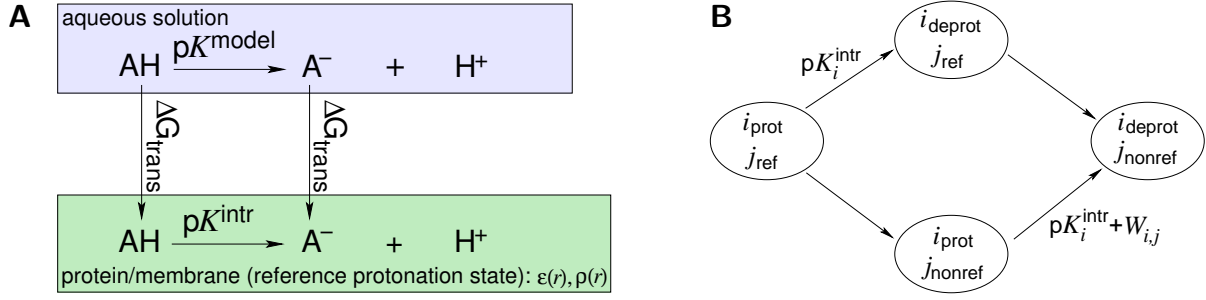


Figure 7. A) Thermodynamic cycle that links the intrinsic pK -value (Eq. 3) to the model compound pK -value (Eq. 7) via the energies associated with the transfer of the protonated (AH) and deprotonated (A^-) form of the model compound from aqueous solution to the protein, in which all other titratable sites are in their reference protonation form. **B)** The interaction energy $W_{i,j}$ is the difference in pK of site i depending on whether site j is in its reference protonation form (Eq. 8). Indices prot and deprot denote the protonated and deprotonated form of site i , respectively. Indices ref and nonref denote the reference and non-reference protonation form of site j , respectively.

$\Delta G_{\text{trans}}(A^-)$ and $\Delta G_{\text{trans}}(AH)$ are the energies to transfer the model compound in its deprotonated and protonated form, respectively, from aqueous solution into the protein environment in its reference protonation state. These transfer energies have two contributions:

$$\Delta G_{\text{trans}} = \Delta G_{\text{Born}} + \Delta G_{\text{back}}. \quad (4)$$

The Born energy contribution ΔG_{Born} is due to the change in the dielectric environment between aqueous solution and the protein: the change of $\epsilon(\vec{r})$ corresponds to a change of the screening of the charges as described above. The Born energy is calculated as

$$\Delta G_{\text{Born}} = \frac{1}{2} \sum_k^K q_k \phi^{\text{protein}}(\vec{r}_k, \rho) - \frac{1}{2} \sum_k^K q_k \phi^{\text{aq}}(\vec{r}_k, \rho), \quad (5)$$

where $\phi^{\text{protein}}(\vec{r}_k, \rho)$ and $\phi^{\text{aq}}(\vec{r}_k, \rho)$ are the potentials evoked by the charge distribution ρ of the model compound at the position \vec{r}_k of the point charge charge q_k in the dielectric environments of the protein and aqueous solution, respectively. The sums run over the K point charges that form the charge distribution ρ of the model compound. The potentials are obtained as solutions of Eq. 1.

The background energy contribution to the transfer energy accounts for the interaction of the charges of the model compound with the so-called background charges in the protein:

$$\Delta G_{\text{back}} = \sum_m^M q_m \phi^{\text{protein}}(\vec{r}_m, \rho). \quad (6)$$

The background charges q_m are the partial charges of atoms for instance in the protein backbone or non-titratable sidechains and the charges of the other titratable sites $j \neq i$

in their reference protonation form $x_j^{(0)}$. $\phi^{\text{protein}}(\vec{r}_m, \rho)$ is the electrostatic potential at the position \vec{r}_m of the background charge q_m due to the charge distribution ρ of the model compound of site i in the dielectric environment of the protein. It can be obtained as solution of Eq. 1. The sum runs over all M background charges m .

The model compound $\text{p}K$ -value characterises the energetics of the protonation equilibrium of the model compound in aqueous solution:

$$\text{p}K^{\text{model}} = -\lg K^{\text{model}} = \Delta G_{\text{deprot}}^{\text{aq}}(\text{AH}), \quad (7)$$

where K^{model} is the equilibrium constant of the protonation equilibrium $\text{AH} \rightleftharpoons \text{A}^- + \text{H}^+$. The model compound $\text{p}K$ -value can be determined experimentally or from quantum chemical calculations.

The pairwise interaction between two sites i and j is assumed to be purely electrostatic and is quantified as the energy of the charge distribution of i in the potential of j . It is calculated as the shift in the intrinsic $\text{p}K$ of site i that is induced by a change in the protonation form of site j from the reference to the non-reference form (Fig. 7B):

$$W_{i,j} = \sum_{k=1}^K \left(q_{k,i}^{\text{prot}} - q_{k,i}^{\text{deprot}} \right) \left(\phi(\vec{r}_k, \rho_j^{\text{ref}}) - \phi(\vec{r}_k, \rho_j^{\text{nonref}}) \right), \quad (8)$$

with $q_{k,i}^{\text{prot}}$ and $q_{k,i}^{\text{deprot}}$ as the partial charges of site i in protonated and deprotonated form, respectively, and ρ_j^{ref} and ρ_j^{nonref} as the charge distributions of site j in its reference and non-reference form, respectively. The summation runs over the K partial charges of site i . $\phi(\vec{r}_k, \rho_j)$ is the potential of the given charge distribution in the protein environment at position \vec{r}_k of partial charge q_k . The electrostatic potentials are again derived from Eq. 1. $W_{i,j}$ is set to zero for $i = j$.

Metropolis Monte Carlo sampling of protonation state energies. From the protonation state energies $G^{(n)}$ in Eq. 2 it is possible to calculate the protonation probability $\langle x_i \rangle$ of a site i at a certain pH:

$$\langle x_i \rangle(\text{pH}) = \frac{\sum_{n=0}^{2^N-1} x_i^{(n)} \exp\left(-\frac{G^{(n)}(\text{pH})}{RT}\right)}{\sum_{n=0}^{2^N-1} \exp\left(-\frac{G^{(n)}(\text{pH})}{RT}\right)}. \quad (9)$$

In order to evaluate this expression, all 2^N protonation state energies $G^{(n)}$ have to be calculated, which is however not feasible in the study of the titration behaviour of proteins with their large number of titratable sites N . Instead, a Metropolis Monte Carlo (MC) approach can be used to sample the protonation state energies. In these simulations, an

initial protonation state vector is randomly chosen and its energy is calculated. Each MC step then consists in randomly changing the protonation form of a single site, that means changing a single component of the protonation state vector $\vec{x}^{(\text{old})}$ from 1 to 0 or from 0 to 1. The energy of the new state $\vec{x}^{(\text{new})}$ is then evaluated and compared to the energy of the old state. Depending on the difference in energy $\Delta G = G^{(\text{new})} - G^{(\text{old})}$ the new state is accepted with a certain probability p according to the Metropolis criterion

$$p = \begin{cases} 1 & \text{if } \Delta G \leq 0, \\ \exp(-\Delta G/RT) & \text{if } \Delta G > 0. \end{cases} \quad (10)$$

During the equilibration phase of an MC simulation, an accepted state is only used as new starting state for the next MC step. During the production phase, protonation states that are accepted are in addition added to an MC output ensemble of protonation states. The probability of a certain protonation state can then be calculated as the probability to find it in the output ensemble of states, and the protonation probability of a certain site $\langle x_i \rangle$ corresponds to the probability to find it to be protonated in the MC output ensemble.

An additional feature enables the MC algorithm to effectively sample the protonation states of strongly interacting sites. Consider a pair of sites i and j for which states (0,1) and (1,0) are low in energy, but states (1,1) and (0,0) have high energies. In this case, starting from state (1,0), state (0,1) can only be reached via two MC steps of which one would cause an increase in energy and would therefore be improbable to be accepted. State (0,1) might therefore never be added to the output ensemble although it is low in energy. To solve this sampling problem, so-called double and triple moves are introduced which simultaneously change the protonation states of two or three sites in one MC step. Double moves are only applied to pairs of sites i and j that have an interaction energy $W_{i,j}$ (Eq. 8) above a certain threshold value W_{double} . Triple moves will be applied to residues i , j and k if $W_{i,j} \geq W_{\text{triple}}$ and $W_{i,k} \geq W_{\text{triple}}$. Normally $W_{\text{triple}} > W_{\text{double}}$ is set.

To obtain a titration curve $\langle x_i \rangle(\text{pH})$, a separate MC simulation has to be run for each pH. Since the resulting curve represents the protonation probability of a site in a multiprotic acid with many interacting titratable sites, it can not be characterised by a single $\text{p}K$ -value [78].

Monte Carlo titration calculations with conformational variability. Most obviously, the Metropolis MC sampling approach is not limited to the protonation state energies given in Eq. 2. If the state energy is formulated to include an energy contribution attributable to different conformational states of the system, MC sampling of the state energies can be used to introduce conformational variability into the otherwise static picture of PBE calculations. For instance, if C different conformations c of the system

are considered, the energy of protonation state n in conformation c can be written as

$$\begin{aligned}
 G^{(n,c)} &= \sum_i^N (x_i^{(n)} - x_i^{(0)}) (\text{pH} - \text{p}K_i^{\text{intr}(c)}) \\
 &+ \frac{1}{2} \sum_i^N \sum_j^N (x_i^{(n)} - x_i^{(0)}) (x_j^{(n)} - x_j^{(0)}) W_{i,j}^{(c)} \\
 &+ G_{\text{conf}}^{(c)}, \tag{11}
 \end{aligned}$$

where $G_{\text{conf}}^{(c)}$ accounts for the relative energies of the different conformations considered. These conformational energies are calculated for the system in its reference protonation state $\vec{x}^{(0)}$. For MC sampling of the state energy in Eq. 11, not only the components of the protonation state vector x_i but also the conformation needs to be randomly changed in order to sample all important states (n, c) .

Molecular mechanics calculations [79] represent one way to obtain the conformational energy differences $G_{\text{conf}}^{(c)}$. In this approach, an empirically parametrised energy function is used to evaluate the energy of a multi-atomic system, depending on the Cartesian coordinates $\vec{x} = x_1, y_1, z_1, \dots, x_A, y_A, z_A$ of all A atoms in the system. The energy function $U(\vec{x})$ is a sum of the potential energies due to the deformation of bonds, angles, dihedral angles or torsion angles, and due to pairwise electrostatic and van der Waals interaction of the atoms:

$$U = U_{\text{bond}} + U_{\text{angle}} + U_{\text{dihedral}} + U_{\text{torsion}} + U_{\text{elec}} + U_{\text{vdW}} \tag{12}$$

U_{dihedral} represents the energy due to rotation of groups around a single bond, and U_{torsion} represents the energy due to out-of-plane positioning of atoms at a double bond. All contributions in Eq. 12 depend on the conformation \vec{x} of the system. For example, the contribution from the covalent bonds is commonly written as

$$U_{\text{bond}}(\vec{x}) = \sum_b^B k_b (d - d_0)^2. \tag{13}$$

Here, d is the distance between two covalently bound atoms, it is defined by the set of atom coordinates \vec{x} . d_0 is the optimal distance between the two atoms, that is the distance at which the potential energy of this bond becomes minimal. k_b is the force constant for the respective bond, which like a spring constant defines the energetic cost of bond deformation. d_0 and k_b are specific for a certain bond as for example a peptide bond between a carbon and a nitrogen atom, and belong to the set of parameters that are empirically determined. The sum runs over all B covalent bonds b in the system. All other terms contributing to the potential energy in Eq. 12 depend in a similar way on the atomic coordinates \vec{x} and a set of empirically determined parameters.

Quantum chemical characterisation of protonation equilibria in vacuum. As outlined above, a protonation equilibrium in a protein environment can be characterised from the shift in the pK -value of an appropriate model compound upon its transfer from aqueous solution into the protein. The model compound pK -values are most commonly derived from experiment. In some cases, however, experimental data are not available, for instance because no suitable model compound can be synthesised. Alternatively, the protonation equilibrium in the protein can in these cases be characterised from a combination of quantum chemical and PBE calculations.

From the quantum chemical calculations described below one can obtain the ground state energies of the protonated model compound $G^{\text{vac}}(\text{AH})$, the deprotonated model compound $G^{\text{vac}}(\text{A}^-)$ and the proton $G^{\text{vac}}(\text{H}^+)$ in vacuum. These quantities enter into the calculation of the deprotonation energy in vacuum according to

$$\begin{aligned} \Delta G_{\text{deprot}}^{\text{vac}} &= G^{\text{vac}}(\text{A}^-) + G^{\text{vac}}(\text{H}^+) - G^{\text{vac}}(\text{AH}) + G^{\text{vib}}(\text{A}^-) + G^{\text{vib}}(\text{AH}) \\ &\quad + G^{\text{translation}}(\text{H}^+) + p\Delta V - T \cdot S(\text{H}^+). \end{aligned} \quad (14)$$

The vibrational energies G^{vib} can be estimated from normal mode analysis [79] of the model compound. $G^{\text{translation}}(\text{H}^+) = \frac{3}{2}RT$ is the translational energy of a proton, the pressure-volume term is estimated to be $p\Delta V = RT$. The entropic contribution $T \cdot S(\text{H}^+)$ is derived from the Sackur-Tetrode equation [80]. From the deprotonation energy in vacuum $\Delta G_{\text{deprot}}^{\text{vac}}$, the deprotonation energy in the protein environment $\Delta G_{\text{deprot}}^{\text{protein}}$ can be obtained from a thermodynamic cycle similar to that of Fig. 7A. The energies ΔG_{trans} to transfer the protonated and deprotonated species from vacuum to the protein environment are obtained from Poisson-Boltzmann calculations. The charge distributions $\rho(\vec{r})$ of the model compound in its two protonation forms are derived from quantum chemical calculations by fitting the potential due to the calculated distribution of nuclei and electrons with atom centred partial charges [81, 82]. The transfer energy of the proton from vacuum to the protein is determined from the potential of the standard hydrogen electrode to be $G_{\text{trans}}(\text{H}^+) = 260.5 \text{ kcal/mol}$ [83].

The energies G^{vac} can for example be obtained from density functional theory (DFT) calculations [84]. DFT represents an approximation to the solution of the time-independent, non-relativistic Schrödinger equation

$$\mathcal{H}\Psi_i = E_i\Psi_i \quad (15)$$

of a given system. The Hamiltonian \mathcal{H} is a differential operator that represents the total energy E_i of a given electronic wave function Ψ_i . Within the framework of the Born-Oppenheimer approximation, which assumes that electrons move in the field of spatially fixed nuclei, the so-called electronic Hamiltonian can be written as

$$\mathcal{H} = \mathcal{T} + \mathcal{V}_{\text{ee}} + \mathcal{V}_{\text{ne}}, \quad (16)$$

where \mathcal{T} represents the kinetic energy of the electrons, \mathcal{V}_{ee} represents the potential energy due to electron-electron interaction, and \mathcal{V}_{ne} represents the potential energy due to electron-nuclei interaction. The solutions of the Schrödinger equation are the electronic wave functions Ψ_i . Of these, the wave function Ψ_0 with the lowest energy E_0 represents the ground state of the system, which is the state of interest in this work. Since it is however impossible to search all possible N -electron wave functions Ψ_i for the ground state wave function Ψ_0 , different approaches have been developed to circumvent this problem.

The basis of DFT are the Hohenberg-Kohn theorems [85], which prove that the ground state electron density does in principle determine all ground-state properties of interest. In analogy to Eq. 16, the ground state energy can be written as a functional of the ground state electron density $\rho_0(\vec{r})$:

$$\begin{aligned} E_0[\rho_0] &= T[\rho_0] + V_{ee}[\rho_0] + V_{ne}[\rho_0] \\ &= F_{\text{HK}}[\rho_0] + V_{ne}[\rho_0]. \end{aligned} \quad (17)$$

In this formulation, the Hohenberg-Kohn functional F_{HK} represents the kinetic energy and electron-electron interaction energy that contribute to the total ground-state energy E_0 of the system. The explicit form of this functional is not known, but approximations have been developed. They are based on the Kohn-Sham approach [86], that introduces a model system which is constructed of N non-interacting electrons and is characterised by the same electron density ρ_0 as the real system. Each of these non-interacting one-electron systems $n = 1, \dots, N$ is characterised by a Schrödinger equation

$$\mathcal{H}_n \Psi_n = E_n \Psi_n. \quad (18)$$

The Hamiltonians of Eq. 18 are written as

$$\mathcal{H}_n = \mathcal{T}_n + \mathcal{V}_{\text{eff}}, \quad (19)$$

where \mathcal{T}_n represent the kinetic energies of the non-interacting electrons, while \mathcal{V}^{eff} needs to be chosen to reproduce ρ_0 of the real system by means of the N non-interacting electrons. The effective energy $V_{\text{eff}}[\rho_0]$ contains the potential energy due to nuclei-electron interaction $V_{ne}[\rho_0]$, the potential energy due to classical electrostatic interaction of the electrons $J[\rho_0]$ and a so-called exchange-correlation energy $V_{xc}[\rho_0]$ of the electrons:

$$V_{\text{eff}}[\rho_0] = V_{ne}[\rho_0] + J[\rho_0] + V_{xc}[\rho_0]. \quad (20)$$

$V_{ne}[\rho_0]$ and $J[\rho_0]$ can be calculated exactly. Approximations remain thus limited to $V_{xc}[\rho_0]$, that represents the remainder of the kinetic energy of the real system that is not accounted for by T_n , and contributions from the non-classical self-interaction, correlation and exchange energies of the electrons. Established approximations to $V_{xc}[\rho_0]$ include the VWN [87] and the PW91 [88] functionals.

3 Synopsis of published and submitted manuscripts

The analysis of the redox-dependent titration behaviour of cytochrome bc_1 is the central issue of this work. However, as outlined in the introduction, cytochrome bc_1 is a complicated system. It has a high number of titratable groups that interact electrostatically with each other and with the redox-active cofactors. The natural environment of the inner mitochondrial membrane needs to be accounted for in the PBE calculations. The Q_o -site shows conformational variability that needs to be considered in the MC titration calculations. In a series of studies, these challenges have been met in simpler systems, and the resulting solutions have then been combined to approach the titration behaviour of cytochrome bc_1 .

As a first approach, the theoretical basis of protonation reactions in mono-, di- and multiprotic acids has been reviewed, and the effect of electrostatic interaction and conformational variability on the titration behaviour of two minimalistic model systems has been carefully characterised. The titration behaviour of a relatively simple soluble protein has then been characterised, taking into account two conformations of a covalently bound chromophore that is itself a titratable group. Calculations on a relatively small CoQ-reducing transmembrane protein, the bacterial photosynthetic reaction centre, support a crystallographically observed pH-dependence of the position of CoQ in the protein's active site. A study of the coupling between protonation and redox reactions in soluble Rieske proteins reveals the structural basis of this catalytically important property of the iron-sulphur cluster. In this way, the work described in Manuscript A to D eventually prepared the grounds for the study of the redox-dependent titration behaviour of cytochrome bc_1 .

Irregular titration behaviour of individual sites in proteins. The highly irregular titration behaviour of several mechanistically important residues in cytochrome bc_1 has motivated a thorough theoretical study about the basis of irregular titration behaviour in proteins (Manuscript A). The article gives an overview of the theory of multi-site titration, including the definition and discussion of microscopic and macroscopic pK -values and the decoupled sites representation of multiprotic acids. It is shown that conformational variability alone can not lead to irregular titration behaviour. In contrast, strong electrostatic interaction between two groups can result in irregular titration behaviour, but only if the two groups titrate in a similar pH-range. This connection is demonstrated using a model system of two titratable sites, where the interaction energies and the difference between the intrinsic pK -values were varied systematically.

A model system consisting of four titratable sites with similar intrinsic pK -values and moderately strong pairwise interaction energies was used to show the effect of mutations in networks of interacting residues. All four residues were consecutively mutated to

non-titratable residues. Some of these mutations had a strong influence on the titration behaviour of the remaining three residues. The effect can be precisely quantified from the calculations but is not intuitively predictable. This result underlines the importance of a thorough theoretical analysis of the titration behaviour of both wildtype and mutant proteins if titratable sites are subject to experimental mutational analysis or even mutational design (Manuscript B).

Coupling between conformational and protonation state changes in asFP.

Manuscript B presents a case where the theoretical characterisation of protonation states in a wildtype protein has been used to prepare the grounds for mutational design. asFP is a fluorescent protein from *Anemonia sulcata* that is of enormous interest for cell biology since it is reversibly photoswitchable and can therefore be used in stimulated emission depletion (STED) microscopy. STED microscopy represents a breakthrough in raster fluorescence microscopy since it allows to locate a fluorescent molecule within a volume element smaller than what would be allowed by the laws of light diffraction. The concept of STED relies on the use of dyes from which fluorescence can be excited by light of wavelength λ_x , and can be depleted by light of wavelength $\lambda_d \neq \lambda_x$. A clever spatial arrangement of excitation and depletion allows to excite the sample in a spot that is smaller than the size dictated by diffraction of the excitatory beam of light.

asFP does in principle represent such a reversibly photoswitchable dye. However, since photoswitching is slow and ineffective, its properties call for improvement by mutational design. A first step in this direction is the characterisation of the switching process at atomic detail. Upon absorption of λ_x , a covalently bound chromophore undergoes a *trans*-to-*cis* transition of a double bond. Since protonation state changes of the chromophore pocket have been proposed to accompany the switching event, the protonation probabilities have been calculated for the wildtype and a mutant of asFP with the chromophore in its *trans* and *cis* configuration. The chromophore itself has two titratable sites and can adopt an anionic, zwitterionic or neutral form. It could be shown that the chromophore in its *trans* configuration is zwitterionic while it is predominantly neutral when it is in the *cis* configuration. The calculated protonation probabilities of the system agree well with an assignment of protonation states based on the comparison of calculated and experimentally determined absorption spectra of the protein.

pH-dependence of the position of CoQ in the the Q_B -site of the photosynthetic reaction centre.

The photosynthetic reaction centre is a transmembrane protein that converts light energy into the chemical energy of reduced CoQ. In the Q_B -site, CoQ gets reduced and is subsequently released in its ubiquinol form. From structural characterisation of the protein it has previously been proposed that the Q_B -pocket comprises two

CoQ binding sites, and that CoQ adopts different conformations depending on the site of binding. The structures of the reaction centre from the purple bacterium *Rhodobacter sphaeroides* reported in Manuscript C show that the position of CoQ in the site depends on pH but that CoQ has the same conformation in both positions. Based on the new structures, we could show from quantum chemical calculations that the energetic barrier between the two positions of CoQ must be small. From PBE/MC titration calculations, the populations of the two positions were quantified as a function of pH yielding results that are consistent with the experimental data. Based on additional new structures obtained for different redox states of the system, the proton uptake upon formation of the semiquinone state of CoQ_B has been determined as a function of pH. Individual residues could be identified that are responsible for the proton uptake.

Coupling between the redox and protonation reactions of the Rieske iron-sulphur cluster. In order to assess the mechanism of CoQ oxidation in the Q_o-site of cytochrome *bc*₁, the protonation and redox reactions of the Rieske iron-sulphur cluster have been characterised (Manuscript D). Two different Rieske proteins have been studied: the soluble fragment of the Rieske subunit of bovine cytochrome *bc*₁ and the Rieske subunit of the biphenyl dioxygenase system from *Burkholderia* sp. The first protein has a high reduction potential, and a redox-dependent protonation state change of its ligand histidines can be observed in the physiological pH-range. The latter protein has a low reduction potential, and its ligand histidines remain protonated at physiological pH regardless of the redox state of the cluster.

A first set of calculations showed that the experimentally determined macroscopic p*K*-values of the Rieske cluster in the two proteins can be accurately reproduced from a combination of PBE and DFT calculations. This agreement demonstrates the power of the combined PBE/DFT approach in characterising the intricate properties of Rieske proteins.

In order to identify the structural basis of the remarkably different properties of the Rieske cluster in the two different proteins, I have performed PBE calculations on a set of mutants of the two proteins. The mutations were chosen such that they remove differences between the two proteins and render them more similar. Taken together, the quantitative analysis of the effect of the studied mutations yields two important results. The removal of hydrogen bonds towards the cluster in the Rieske protein from cytochrome *bc*₁ leads to an increase of its p*K*-values. The effect is however small compared to the difference in p*K*-values of the two wildtype proteins. In contrast, the removal of four negatively charged residues in the Rieske subunit of the bacterial oxygenase system leads to a pronounced decrease of the p*K*-values, yielding an effect that is in total larger than that of the removal of the hydrogen bonds. Since the negative charges are not even in closest proximity to

the cluster, this result demonstrates that long range electrostatic interactions must not be neglected in computational approaches to enzyme mechanisms. The effect of hydrogen bonds in the high-potential Rieske protein and of the negative charges in the low-potential Rieske protein taken together account fully for the difference in macroscopic pK -values of the cluster in the two proteins.

Redox-linked protonation state changes in cytochrome bc_1 . In its two CoQ binding active sites, cytochrome bc_1 catalyses the combined oxidation/deprotonation and reduction/protonation of CoQ. Redox-linked protonation state changes of the protein must thus be an essential element of the catalytic mechanism. Within the last couple of years, several studies have been published that use redox-induced FTIR difference spectroscopy to characterise such redox-linked protonation state changes. While protonation state changes could indeed be observed, their assignment to specific residues is complicated or impossible. By performing PBE calculations, the protonation probabilities of all titratable sites in completely reduced and completely oxidised cytochrome bc_1 from *S. cerevisiae* have been quantified (Manuscript E and F). Redox-linked protonation state changes of individual residues could be identified from comparison of the results for the two redox states. These results could be linked to data obtained from FTIR experiments. Two crystallographically observed conformations of the Q_o -site have been included in the MC titration calculations. MC sampling of the protonation and conformational states allows to identify possible redox-linked conformational changes of the system.

In the Q_i -site, the direct ligands of CoQ could be shown to have a higher protonation probability in the reduced than in the oxidised state. The proposed function of these residues as proton donor groups in the CoQ reduction reaction could thus be confirmed. A cluster of lysine residues with redox-dependent and strongly correlated protonation probabilities could be identified. This lysine cluster has been proposed to be responsible for proton uptake to the Q_i -site. The strong interaction between the residues in this cluster is the reason for the partly highly unusual shape of their protonation probability curves (Manuscript A). A cardiolipin molecule that is bound close to the Q_i -site could be shown to be doubly deprotonated and negatively charged over the whole pH-range studied in both redox states of the system. In contrast to previously proposed ideas, the cardiolipin molecule is thus most likely not involved in proton uptake to the site but helps to increase the protonation probability in the lysine cluster.

In the Q_o -site, a probable position of CoQ in the site has been determined from the position of stigmatellin in the site, and from structural information about the relative orientation of CoQ and stigmatellin in the structurally similar Q_B -site of the photosynthetic reaction centre (Manuscript C). This protein has been crystallised once with the inhibitor and once with CoQ. The population of the two conformations of E272^{CYB} in the Q_o -site is

redox-dependent. However, since one and the same conformation is predominantly populated in the two studied redox states (to 100 % in the oxidised state and to about 60 % in the reduced state), the results do not allow to decide whether a conformational change of the site occurs during turnover. The observed protonation pattern of E272^{CYB} in the different conformations is consistent with a previously proposed role of this residue in the gating of CoQ oxidation. The Rieske cluster could be shown to undergo redox-linked protonation state changes in the physiological pH-range also in the context of the Q_o-site with CoQ bound. A redox-linked protonation state change of one of the propionate moieties of haem *b_L* supports the previously proposed idea that electron transfer from CoQ to haem *b_L* is accompanied by transfer of a proton from the Q_o-site to one of the propionate groups of haem *b_L*. A similar but weaker redox-linked protonation state change could be observed for one of the propionate moieties of haem *c₁*.

Taken together, the identified redox-linked protonation state changes are in agreement with the available FTIR data. Only the puzzling coupling between the oxidation of haem *b_L* and protonation of a carboxylic sidechain observed in one of the FTIR studies is not consistent with the calculation results. The theoretical study helps to assign the observed redox-linked changes in the FTIR spectra to individual titratable sites in the large protein complex.

Bibliography

- [1] W. A. Cramer and D. B. Knaff (1991): *Energy transduction in biological membranes*. Springer-Verlag, Heidelberg
- [2] P. Mitchell (1961): Coupling of phosphorylation to electron and hydrogen transfer by a chemi-osmotic type of mechanism. *Nature* 191, 144–148
- [3] M. Saraste (1999): Oxidative phosphorylation at the fin de siècle. *Science* 283, 1488–1493
- [4] E. C. Slater (2003): Keilin, cytochrome, and the respiratory chain. *J. Biol. Chem.* 278, 16455–16461
- [5] S. de Vries, S. P. J. Albracht, J. A. Berden and E. C. Slater (1981): A new species of bound semiquinone anion in QH₂:cytochrome *c* oxidoreductase. *J. Biol. Chem.* 256, 11996–11998
- [6] S. Jünemann, P. Heathcote and P. R. Rich (1998): On the mechanism of quinol oxidation in the *bc*₁ complex. *J. Biol. Chem.* 273, 21603–21607
- [7] P. Mitchell (1976): Possible molecular mechanism of the protonmotive function of cytochrome systems. *J. Theor. Biol.* 62, 327–367
- [8] A. R. Crofts (2004): The Q-cycle — a personal perspective. *Photosynth. Res.* 80, 223–243
- [9] B. L. Trumpower (1990): The protonmotive Q cycle. Energy transduction by coupling of proton translocation to electron transfer by the cytochrome *bc*₁ complex. *J. Biol. Chem.* 265, 11409–11412
- [10] C. Hunte, J. Koepke, C. Lange, T. Roßmanith and H. Michel (2000): Structure at 2.3 Å of the cytochrome *bc*₁ complex from the yeast *Saccharomyces cerevisiae* co-crystallized with an antibody Fv fragment. *Structure* 8, 669–684
- [11] C. Lange, J. H. Nett, B. L. Trumpower and C. Hunte (2001): Specific roles of protein-lipid interactions in the yeast cytochrome *bc*₁ complex structure. *EMBO J.* 20, 6591–6600
- [12] H. Palsdottir, C. G. Lojero, B. L. Trumpower and C. Hunte (2003): Structure of the yeast cytochrome *bc*₁ with a hydroxyquinone anion Q_o site inhibitor bound. *J. Biol. Chem.* 278, 31303–31311
- [13] H. Palsdottir and C. Hunte (2004): Lipids in membrane protein structures. *Biochim. Biophys. Acta* 1666, 2–18
- [14] C. Hunte (2001): Insights from the structure of the yeast cytochrome *bc*₁ complex: crystallization of membrane proteins with antibody fragments. *FEBS Lett.* 504, 126–132
- [15] M. E. Schmitt and B. L. Trumpower (1990): Subunit 6 regulates half of the sites reactivity of the dimeric cytochrome *bc*₁ complex in *Saccharomyces cerevisiae*.

- J. Biol. Chem.* 256, 17005–17011
- [16] B. L. Trumpower (2002): A concerted alternating sites mechanism of ubiquinol oxidation by the dimeric cytochrome bc_1 complex. *Biochim. Biophys. Acta* 1555, 166–173
- [17] R. Covián, E. B. Gutierrez-Cirlos and B. L. Trumpower (2004): Anti-cooperative oxidation of ubiquinol by the yeast cytochrome bc_1 complex. *J. Biol. Chem.* 279, 15040–15049
- [18] X. Gong, L. Yu, D. Xia and C.-A. Yu (2005): Evidence for electron equilibrium between the two hemes b_L in the dimeric cytochrome bc_1 complex. *J. Biol. Chem.* 280, 9251–9257
- [19] R. Covián and B. L. Trumpower (2005): Rapid electron transfer between monomers when the cytochrome bc_1 complex dimer is reduced through center N. *J. Biol. Chem.* 280, 22732–33740
- [20] H. I. Silman, J. S. Rieske, S. H. Lipton and H. Baum (1967): A new protein component of complex III of the mitochondrial electron transfer chain. *J. Biol. Chem.* 242, 4867–4875
- [21] U. Schulte, M. Arretz, H. Schneider, M. Tropschug, E. Wachter, W. Neupert and H. Weiss (1989): A family of mitochondrial proteins involved in bioenergetics and biogenesis. *Nature* 339, 147–149
- [22] X. Gao, X. Wen, L. Esser, B. Quinn, L. Yu, C.-A. Yu and D. Xia (2003): Structural basis for the quinone reduction in the bc_1 complex: a comparative analysis of crystal structures of mitochondrial cytochrome bc_1 with bound substrate and inhibitors at the Q_i site. *Biochemistry* 42, 9067–9080
- [23] Z. Zhang, L. Huang, V. M. Shulmeister, Y.-I. Chi, L. L. Lim, L.-W. Hung, A. R. Crofts, E. A. Berry and S.-H. Kim (1998): Electron transfer by domain movement in cytochrome bc_1 . *Nature* 392, 677–684
- [24] L. Huang, D. Cobessi, E. Y. Tung and E. A. Berry (2005): Binding of the respiratory chain inhibitor antimycin to the mitochondrial bc_1 complex: a new crystal structure reveals an altered intramolecular hydrogen-bonding pattern. *J. Mol. Biol.* 2005, 573–597
- [25] D. R. J. Kolling, R. I. Samoilova, J. T. Holland, E. A. Berry, S. A. Dikanov and A. R. Crofts (2003): Exploration of ligands to the Q_i site semiquinone in the bc_1 complex using high-resolution EPR. *J. Biol. Chem.* 278, 39747–39754
- [26] S. A. Dikanov, R. I. Samoilova, D. R. Kolling, J. T. Holland and A. R. Crofts (2004): Hydrogen bonds involved in binding the Q_i -site semiquinone in the bc_1 complex, identified through deuterium exchange using pulsed EPR. *J. Biol. Chem.* 279, 15814–15823
- [27] B. Gomez and N. C. Robinson (1999): Phospholipase digestion of bound cardiolipin inactivates bovine cytochrome bc_1 . *Biochemistry* 38, 9031–9038

- [28] M. Schlame, D. Rua and M. L. Greenberg (2000): The biosynthesis and functional role of cardiolipin. *Prog. Lipid. Res.* 39, 257–288
- [29] C. Hunte, H. Palsdottir and B. L. Trumpower (2003): Protonmotive pathways and mechanisms in the protonmotive cytochrome bc_1 complex. *FEBS Lett.* 545, 39–46
- [30] E. A. Berry, M. Guergova-Kuras, L. Huang and A. R. Crofts (2000): Structure and function of cytochrome bc complexes. *Annu. Rev. Biochem.* 69, 1005–1075
- [31] A. R. Crofts (2004): The cytochrome bc_1 complex: function in the context of structure. *Annu. Rev. Physiol.* 66, 689–733
- [32] A. Y. Mulkidjanian (2005): Ubiquinol oxidation in the cytochrome bc_1 complex: reaction mechanism and prevention of short-circuiting. *Biochim. Biophys. Acta* 1709, 5–34
- [33] S. Iwata, J. W. Lee, K. Okada, J. K. Lee, M. Iwata, B. Rasmussen, T. A. Link, S. Ramaswamy and B. K. Jap (1998): Complete structure of the 11-subunit bovine mitochondrial cytochrome bc_1 complex. *Science* 281, 64–71
- [34] C. Lange and C. Hunte (2002): Crystal structure of the yeast cytochrome bc_1 complex with its bound substrate cytochrome c . *Proc. Natl. Acad. Sci.* 99, 2800–2805
- [35] X. Gao, X. Wen, C.-A. Yu, L. Esser, S. Tsao, B. Quinn, L. Zhang, L. Yu and D. Xia (2002): The crystal structure of mitochondrial cytochrome bc_1 in complex with famoxadone: the role of aromatic-aromatic interaction in inhibition. *Biochemistry* 42, 11692–11702
- [36] L. Esser, B. Quinn, Y.-F. Li, M. Zhang, M. Elberry, L. Yu, C.-A. Yu and D. Xia (2004): Crystallographic studies of quinol oxidation site inhibitors: a modified classification of inhibitors for the cytochrome bc_1 complex. *J. Mol. Biol.* 341, 281–302
- [37] E. A. Berry, L.-S. Huang, L. K. Saechao, N. G. Pon, M. Valkova-Valchanova and F. Daldal (2004): X-ray structure of *Rhodobacter capsulatus* cytochrome bc_1 : comparison with its mitochondrial counterparts. *Photosynth. Res.* 81, 251–275
- [38] R. I. Samoilova, D. Kolling, T. Uzawa, T. Iwasaki, A. R. Crofts and S. A. Dikanov (2001): The interaction of the Rieske iron-sulfur protein with occupants of the Q_o site of the bc_1 complex, probed by electron spin echo envelope modulation. *J. Biol. Chem.* 277, 4605–4608
- [39] U. Brandt and G. von Jagow (1991): Analysis of inhibitor binding to the mitochondrial cytochrome c reductase by fluorescence quench titration. *Eur. J. Biochem.* 195, 163–170
- [40] A. R. Crofts, B. Barquera, R. B. Gennis, R. Kuras, M. Guergova-Kuras and E. A. Berry (1999): Mechanism of ubiquinol oxidation by the bc_1 complex: different domains of the quinol binding pocket and their role in the mechanism and binding of inhibitors. *Biochemistry* 38, 15807–15826
- [41] H. Ding, D. E. Robertson, F. Daldal and P. L. Dutton (1992): Cytochrome bc_1

- complex [2Fe-2S] cluster and its interaction with ubiquinone and ubihydroquinone at the Q_o site: a double occupancy model. *Biochemistry* 31, 3144–3158
- [42] H. Ding, C. C. Moser, D. E. Robertson, M. K. Tokito, F. Daldal and P. L. Dutton (1995): Ubiquinone pair in the Q_o site central to the primary energy conversion of cytochrome *bc*₁ complex. *Biochemistry* 34, 15979–15996
- [43] R. E. Sharp, C. C. Moser, B. R. Gibney and P. L. Dutton (1999): Primary steps in the energy conversion reaction of the cytochrome *bc*₁ complex Q_o site. *J. Bioenerg. Biomemb.* 31, 225–223
- [44] S. Bartoschek, M. Johansson, B. H. Geierstanger, J. G. Okun, C. R. D. Lancaster, E. Humpfer, L. Yu, C.-A. Yu, C. Griesinger and U. Brandt (2001): Three molecules of ubiquinone bind specifically to the mitochondrial cytochrome *bc*₁ complex. *J. Biol. Chem.* 276, 35231–35234
- [45] T. A. Link (1997): The role of the 'Rieske' iron sulfur protein in the hydroquinone oxidation (Q_P) site of cytochrome *bc*₁ complex. The proton gated affinity change mechanism. *FEBS Lett.* 412, 257–264
- [46] N. B. Ugulava and A. R. Crofts (1998): CD-monitored redox titration of the Rieske Fe-S protein of *Rhodobacter sphaeroides*: pH dependence of the midpoint potential in isolated *bc*₁ complex and in membranes. *FEBS Lett.* 440, 409–413
- [47] M. Guergova-Kuras, R. Kuras, N. Ugulava, I. Hadad and A. R. Crofts (2000): Specific mutagenesis of the Rieske iron-sulfur protein in *Rhodobacter sphaeroides* shows that both the thermodynamic gradient and the p*K* of the oxidized form determine the rate of ubiquinol oxidation by the *bc*₁ complex. *Biochemistry* 39, 7436–7444
- [48] B. Gurung, L. Yu, D. Xia and C.-A. Yu (2005): The iron-sulfur cluster of the Rieske iron sulfur protein functions as a proton exiting gate in the cytochrome *bc*₁ complex. *J. Biol. Chem.* 280, 24895–24902
- [49] A. R. Crofts, S. Hong, N. Ugulava, B. Barquera, R. Gennis, M. Guergova-Kuras and E. A. Berry (1999): Pathways for proton release during ubihydroquinone oxidation by the *bc*₁ complex. *Proc. Natl. Acad. Sci. USA* 96, 10021–10026
- [50] P. R. Rich (2004): The quinone chemistry of *bc* complexes. *Biochim. Biophys. Acta* 1658, 165–171
- [51] T. Wenz, P. Hellwig, F. MacMillan, B. Meunier and C. Hunte (2006): Probing the role of E272 in quinol oxidation of mitochondrial complex III. *Biochemistry* 45, 9042–9052
- [52] A. Osyczka, H. Zhang, C. Mathé, P. R. Rich, C. C. Moser and P. L. Dutton (2006): Role of the PEWY glutamate in hydroquinone–quinone oxidation–reduction catalysis in the Q_o site of cytochrome *bc*₁. *Biochemistry* 45, 10492–10503
- [53] A. Osyczka, C. C. Moser, F. Daldal and P. L. Dutton (2004): Reversible redox energy coupling in electron transfer chains. *Nature* 427, 607–612

- [54] A. Osyczka, C. C. Moser and P. L. Dutton (2005): Fixing the Q cycle. *Trends Biochem. Sci.* *30*, 176–182
- [55] F. Muller, A. R. Crofts and D. M. Kramer (2002): Multiple Q-cycle bypass reactions at the Q_o site of the cytochrome *bc*₁ complex. *Biochemistry* *41*, 7866–7874
- [56] Q. Chen, Q. J. Vazquez, S. Moghaddas, C. L. Hoppel and E. J. Lesnefsky (2003): Production of reactive oxygen species by mitochondria. Central role of complex III. *J. Biol. Chem.* *278*, 35027–26031
- [57] S. Moghaddas, C. L. Hoppel and E. J. Lesnefsky (2003): Aging defect at the Q_o site of complex III augments oxyradical production in the rat heart interfibrillary mitochondria. *Archives. Biochem. Biophys.* *414*, 59–66
- [58] J. Sun and B. L. Trumpower (2003): Superoxide generation by the cytochrome *bc*₁ complex. *Arch. Biochem. Biophys.* *419*, 198–206
- [59] F. L. Muller, Y. Liu and H. van Remmen (2004): Complex III releases superoxide to both sides of the inner mitochondrial membrane. *J. Biol. Chem.* *279*, 49064–49073
- [60] J. L. Cape, J. R. Strahan, M. J. Lenaeus, B. A. Yuknis, T. T. Le, J. N. Shepherd, M. K. Bowman and D. M. Kramer (2005): The respiratory substrate rhodoquinol induces Q-cycle bypass reactions in the yeast cytochrome *bc*₁ complex: mechanistic and physiological implications. *J. Biol. Chem.* *280*, 34654–34660
- [61] A. R. Crofts, S. Lhee, S. B. Crofts, J. Cheng and S. Rose (2006): Proton pumping in the *bc*₁ complex: a new gating mechanism that prevents short circuits. *Biochim. Biophys. Acta* *1757*, 1019–1034
- [62] K. Xiao, L. Yu and C. Yu (2000): Confirmation of the involvement of protein domain movement during the catalytic cycle of the cytochrome *bc*₁ complex by the formation of an intersubunit disulfide bond between cytochrome *b* and the iron-sulfur protein. *J. Biol. Chem.* *275*, 38597–38604
- [63] E. Darrouzet, C. C. Moser, P. L. Dutton and F. Daldal (2001): Large scale domain movement in cytochrome *bc*₁: a new device for electron transfer in proteins. *Trends Biochem. Sci.* *26*, 445–451
- [64] S. Izrailev, A. R. Crofts, E. A. Berry and K. Schulten (1999): Steered molecular dynamics simulation of the Rieske subunit motion in the cytochrome *bc*₁ complex. *Biophys. J.* *77*, 1753–1768
- [65] E. Darrouzet, M. Valkova-Valchanova, C. C. Moser, P. L. Dutton and F. Daldal (2000): Uncovering the [2Fe2S] domain movement in cytochrome *bc*₁ and its implications for energy conversion. *Proc. Natl. Acad. Sci.* *97*, 4567–4572
- [66] E. Darrouzet, M. Valkova-Valchanova and F. Daldal (2000): Probing the role of the Fe-S subunit hinge region during Q_o site catalysis in *Rhodobacter capsulatus bc*₁ complex. *Biochemistry* *39*, 15475–15483
- [67] J. H. Nett, C. Hunte and B. L. Trumpower (2000): Changes to the length of the

- flexible linker region of the Rieske protein impair the interaction of ubiquinol with the cytochrome bc_1 complex. *Eur. J. Biochem.* 267, 5777–5782
- [68] R. C. Sadoski, G. Engstrom, H. Tian, L. Zhang, C.-A. Yu, L. Yu, B. Durham and F. Millett (2000): Use of a photoactivated ruthenium dimer complex to measure electron transfer between the Rieske iron-sulfur protein and cytochrome c_1 in the cytochrome bc_1 complex. *Biochemistry* 39, 4231–4236
- [69] M. Brugna, S. Rodgers, A. Schricker, G. Montoya, M. Kazmeier, W. Nitschke and I. Sinning (2000): A spectroscopic method for observing the domain movement of the Rieske iron-sulfur protein. *Proc. Natl. Acad. Sci.* 97, 2069–2074
- [70] A. R. Crofts, V. P. Shinkarev, S. A. Dikanov, R. I. Samoilova and D. Kolling (2002): Interactions of quinone with the iron-sulfur protein of the bc_1 complex: is the mechanism spring-loaded? *Biochim. Biophys. Acta* 1555, 48–53
- [71] E. Darrouzet, M. Valkova-Valchanova and F. Daldal (2002): The [2Fe-2S] cluster E_m as an indicator of the iron-sulfur subunit position in the ubihydroquinone oxidation site of the cytochrome bc_1 complex. *J. Biol. Chem.* 277, 3464–3470
- [72] J. W. Cooley, A. G. Roberts, M. K. Bowman, D. M. Kramer and F. Daldal (2004): The raised midpoint potential of the [2Fe2S] cluster of cytochrome bc_1 is mediated by both the Q_o site occupants and the head domain position of the Fe-S subunit. *Biochemistry* 43, 2217–2227
- [73] H. Kim, D. Xia, C.-A. Yu, J.-Z. Xia, A. M. Kachurin, L. Zhang, L. Yu and J. Deisenhofer (1998): Inhibitor binding changes domain mobility in the iron-sulfur protein of the mitochondrial bc_1 complex from bovine heart. *Proc. Natl. Acad. Sci. USA* 95, 8026–8033
- [74] L. Esser, X. Gong, S. Yang, L. Yu, C.-A. Yu and D. Xia (2006): Surface-modulated motion switch: capture and release of iron-sulfur protein in the cytochrome bc_1 complex. *Proc. Natl. Acad. Sci.* 103, 13045–13050
- [75] A. Warshel, P. K. Sharma, M. Kato, Y. Xiang, H. Liu and M. H. M. Olsson (2006): Electrostatic basis for enzyme catalysis. *Chem. Rev.* 106, 3210–3235
- [76] G. M. Ullmann and E.-W. Knapp (1999): Electrostatic models for computing protonation and redox equilibria in proteins. *Eur. Biophys. J.* 28, 533–551
- [77] N. Calimet and G. M. Ullmann (2004): The effect of a transmembrane pH gradient on protonation probabilities of bacteriorhodopsin. *J. Mol. Biol.* 339, 571–589
- [78] G. M. Ullmann (2003): Relations between protonation constants and titration curves in polyprotic acids: A critical view. *J. Phys. Chem. B* 107, 1263–1271
- [79] A. R. Leach (2001): *Molecular modelling*. Prentice hall, Harlow
- [80] T. Hill (1960): *An introduction to statistical thermodynamics*. Addison-Wesley, Reading, Massachusetts
- [81] L. M. Chirlian and M. Miller Fracl (1987): Atomic charges derived from electrostatic

- potentials: a detailed study. *J. Comput. Chem.* 8, 894–905
- [82] C. M. Breneman and K. B. Wiberg (1989): Determining atom-centered monopoles from molecular electrostatic potentials. The need for high spin sampling density in formamide conformational analysis. *J. Comput. Chem.* 11, 361–373
- [83] H. Reiss and A. Heller (1985): The absolute potential of the standard hydrogen electrode: a new estimate. *J. Phys. Chem.* 89, 4207–4213
- [84] M. C. Holthausen and W. Koch (2000): *A chemist's guide to density functional theory*. Wiley-VCH, Weinheim
- [85] P. Hohenberg and W. Kohn (1964): Inhomogenous electron gas. *Phys. Rev.* 136, B864–B871
- [86] W. Kohn and L. J. Sham (1965): Self consistent equations including exchange and correlation effects. *Phys. Rev.* 40, A1133–A1138
- [87] S. H. Vosko, L. Wilk and M. Nusair (1980): Accurate spin-dependent electron liquid correlation energies for local spin density calculations: a critical analysis. *Can. J. Phys.* 58, 1200–1211
- [88] J. P. Perdew, J. A. Chevary, S. H. Vosko, K. A. Jackson, M. R. Pederson, D. J. Singh and C. Fiolhais (1992): Atoms, molecules, solids, and surfaces: applications of the generalized gradient approximation for exchange and correlation. *Phys. Rev. B* 46, 6671–6687

List of published and submitted manuscripts

- A.** Astrid R. Kligen, Elisa Bombarda and G. Matthias Ullmann (2006): Theoretical investigation of the behavior of titratable groups in proteins. *Photochem. Photobiol. Sci.* 5, 588-596

Calculations on the model systems presented in this article were run by Matthias Ullmann and myself. The results were analysed and interpreted by Matthias Ullmann and myself. The manuscript was written by Matthias Ullmann and myself together with Elisa Bombarda.

- B.** Lars V. Schäfer, Gerrit Groenhof, Astrid R. Kligen, G. Matthias Ullmann, Martial Boggio-Pasqua, Michael A. Robb and Helmut Grubmüller (2006): Photoswitching of the fluorescent protein asFP: mechanism, proton pathways, and absorption spectra. *Angew. Chem. Int. Ed.*, in press

All PBE calculations described in this manuscript were performed by myself. The results from these calculations were analysed by myself together with Matthias Ullmann. The molecular dynamics simulations were run by Lars Schäfer and Gerrit Groenhof. The quantum chemical calculations were performed by Lars Schäfer and Martial Boggio-Pasqua together with Gerrit Groenhof, Michael Robb and Helmut Grubmüller. The manuscript was written by Lars Schäfer and myself together with Gerrit Groenhof and Helmut Grubmüller.

- C.** Jürgen Koepke, Eva-Maria Krammer, Astrid R. Kligen, Pierre Sebban, G. Matthias Ullmann and Günther Fritzsche (2006): pH modulates the quinone position in the photosynthetic reaction-center from *Rhodobacter sphaeroides* in the neutral and charge separated states. Submitted to *Structure*

The X-ray structures reported in this manuscript were solved by Jürgen Koepke and Günther Fritzsche. The corresponding parts of the manuscript were written by Jürgen Koepke together with Günther Fritzsche and Pierre Sebban. All reported calculations were run by Eva-Maria Krammer with support from my side. The results were analysed and interpreted by Eva-Maria Krammer, Matthias Ullmann, Pierre Sebban and myself. The corresponding parts of the manuscript were prepared by Eva-Maria Krammer together with Matthias Ullmann and me.

- D.** Astrid R. Kligen and G. Matthias Ullmann (2003): Negatively charged residues and hydrogen bonds tune the ligand histidine pK_a values of Rieske iron-sulfur proteins. *Biochemistry* 43, 12383-12389

All calculations described in the manuscript were performed by myself. Results

were discussed and analysed by Matthias Ullmann and myself. The manuscript was prepared by myself together with Matthias Ullmann.

- E.** Astrid R. Kligen, Hildur Palsdottir, Carola Hunte and G. Matthias Ullmann (2006): Redox-linked protonation state changes in cytochrome bc_1 . I. The Q_i -site. Submitted to *Biochim. Biophys. Acta*

All calculations described in this manuscript were performed by myself. The calculations are based on structures solved by Hildur Palsdottir and Carola Hunte. The manuscript was prepared by myself together with Matthias Ullmann and Carola Hunte.

- F.** Astrid R. Kligen, Hildur Palsdottir, Carola Hunte and G. Matthias Ullmann (2006): Redox-linked protonation state changes in cytochrome bc_1 . II. The Q_o -site and cytochrome c_1 . Submitted to *Biochim. Biophys. Acta*

All calculations described in this manuscript were performed by myself. The calculations are based on structures solved by Hildur Palsdottir and Carola Hunte. The manuscript was prepared by myself together with Matthias Ullmann and Carola Hunte.

Manuscript A

Theoretical investigation of the behavior of titratable groups in proteins

Astrid R. Klungen, Elisa Bombarda and G. Matthias Ullmann

Photochem. Photobiol. Sci. 5, 588-596 (2006)

Manuscript B

Lars V. Schäfer, Gerrit Groenhof, Astrid R. Klungen, G. Matthias Ullmann,
Martial Boggio-Pasqua, Michael A. Robb and Helmut Grubmüller

Photoswitching of the fluorescent protein asFP:
mechanism, proton pathways, and absorption spectra

Angew. Chem. Int. Ed., in press

Manuscript C

Jürgen Koepke, Eva-Maria Krammer, Astrid R. Klinge, Pierre Sebban,
G. Matthias Ullmann and Günther Fritzsche

pH modulates the quinone position in the photosynthetic reaction-center from
Rhodobacter sphaeroides in the neutral and charge separated states

Submitted to *Structure*

Manuscript D

Astrid R. Klingen and G. Matthias Ullmann

Negatively charged residues and hydrogen bonds tune the ligand histidine pK_a values
of Rieske iron-sulfur proteins

Biochemistry 43, 12383-12389 (2004)

Manuscript E

Astrid R. Klingen, Hildur Palsdottir, Carola Hunte and G. Matthias Ullmann

Redox-linked protonation state changes in cytochrome bc_1 .

I. The Q_i -site

Submitted to *Biochim. Biophys. Acta*

Manuscript F

Astrid R. Klingen, Hildur Palsdottir, Carola Hunte and G. Matthias Ullmann

Redox-linked protonation state changes in cytochrome bc_1 .

II. The Q_o -site and cytochrome c_1

Submitted to *Biochim. Biophys. Acta*